Int. J. Heat Mass Transfer. Vol. 36, No. 4, pp. 907–918, 1993
Printed in Great Britain

0017–9310/93 $6.00 + 0.00

Experimental measurements of large-scale temperature fluctuation structures in a heated incompressible turbulent boundary layer

NADER BAGHERI
Department of Engineering, California Maritime Academy, Vallejo, CA 94590, U.S.A.

and

BRUCE R. WHITE
Department of Mechanical, Aeronautical, and Material Engineering, University of California, Davis, CA 95616, U.S.A.

(*Received* 20 *August* 1991 *and in revised form* 11 *May* 1992)

Abstract—Hot-wire anemometry measurements over a heated flat plate are made for three different temperature difference cases of 10, 15, and 20°C. Space–time correlations of temperature fluctuations T' are determined from which mean convection velocities, mean inclination angles, extent in space, and coherence characteristics of T' large-scale structure are calculated. The T' mean convection velocity is found as a function of y^+. The T' structure inclination angle is 30 deg. The T' structure is limited to the viscous defect length in the normal and spanwise directions. However, in the streamwise direction, the structure is mildly dependent on the temperature difference.

INTRODUCTION

THE PRESENT study is an experimental investigation of a developing turbulent boundary layer over a heated flat plate. The characteristics and structure of the flow were investigated through a series of space–time correlation measurements. The objective of this study was to enhance understanding of the physics of heat transfer occurring in the turbulent boundary layer.

During the last decade much attention has been given to the study of coherent structures in turbulent flows. Turbulence contains large-scale coherent structures which have dimensions comparable with the size of the boundary layer. These large-scale coherent structures have a large correlation over a significant region of the boundary layer. Therefore, space–time correlation methods have been used to investigate these structures. It was first through flow visualization experiments that large-scale structures were observed. Later, space–time correlation measurements of the large-scale motions correlated the structures' shape and motion. The large-scale motions were found to be three-dimensional, elongated in the streamwise direction, and the outermost non-turbulent fluid appeared to ride over the turbulent/non-turbulent interface.

Space–time correlation methods have been and continue to be an important tool in understanding the physics of the turbulent boundary layer. The time- and length-scales of turbulent flows may be determined by these correlations which are measures of temporal and spatial coherence of turbulent structures responsible for the bulk of heat and momentum transports.

The space–time correlation measurements of velocity fluctuations for isothermal flows have been carried out by many investigators. Kline and Robinson [1] organized a community-wide survey and evaluated the coherent structures and motions in isothermal turbulent boundary layers. In their survey they defined the state of the turbulence structure knowledge. In 1989, Strataridakis *et al.* [2] obtained the space–time correlation of the u' and v' velocities and $u'v'$ using a pair of $\times$-wire subminiature probes. They obtained the mean convection velocities, the mean inclination angles, and the spatial extent of the u', v', and $u'v'$ large-scale structures. In the present work, comparisons of the thermal structures are made to the results of Strataridakis *et al.*

For non-isothermal flow, however, there is not much work reported in the literature. Recently, Bagheri *et al.* [3] reported the direct measurement of turbulent Prandtl number and also presented some preliminary results of thermal structure measurements. In the current work, an extension of our earlier preliminary measurements, a two-dimensional turbulent boundary layer developing on a smooth heated surface in zero-pressure-gradient flow with an unheated starting length is investigated. The objective of the study was to obtain two-point correlations to the temperature fluctuation measurements for the calculations

NOMENCLATURE

C_f	friction coefficient
k	thermal conductivity
$R_{T,T}$	cross-correlation coefficient
St	Stanton number
t	time
T	temperature
u	instantaneous streamwise velocity
U	time-mean average streamwise velocity
u^*	friction velocity
v	instantaneous normal velocity
x	streamwise direction
y	normal direction
z	spanwise direction.

Greek symbols

δ	hydrodynamic boundary-layer thickness
δ_T	thermal boundary-layer thickness
$\Delta 2$	enthalpy thickness
θ	momentum thickness
ν	kinematic viscosity
ρ	density.

Superscripts

$'$	fluctuating quantity
$+$	normalization with viscous units, u^* and ν.

Subscripts

∞	freestream
c	convection velocity
rms	root-mean-square
w	wall.

of the mean convection velocity, the mean inclination angle, and the $R_{T,T}$ isocorrelation contours for both the streamwise and spanwise directions for a limited range of non-dimensional wall heating coefficients. From the $R_{T,T}$ contours the streamwise and lateral size of the thermal structures were determined.

EXPERIMENTAL FACILITY

The experiments were carried out in an open-return-type wind tunnel, Fig. 1(a), with an overall length of 7.5 m. The entrance section had a 13.6:1 contraction ratio with a bell-mouth shape. Air filter, Hexcel honeycomb, and six screens were placed at the entrance of the converging section in order to remove the dust particles, straighten the flow and reduce the freestream turbulence level, which was about 1.5%.

The test section of the tunnel was 3.04 m long, 0.304 m high and 0.304 m wide. This section was designed to provide a zero-pressure-gradient environment. The freestream velocity ranged from 2.5 to 25 m s^{-1}. Access to the test section was through four Plexiglas doors, two on each side of the test section. The four internal corners in the test section had 5 cm radius fillets installed to reduce secondary corner flows. Additional sealing was achieved by taping the Plexiglas doors to the test section from the sides.

The diffuser section was 2.26 m long and had an expansion area that provided a continuous transition from the rectangular cross-section area of the test section to a circular cross-section of the fan. The converging and the diffuser sections were both attached to the test section. A thick rubber interface seal connected the diffuser section to the fan/motor drive system. The rubber internal seal acted as a shock absorber and prevented the fan vibration being transferred to the main body of the wind tunnel [4].

The fan had nine constant pitch blades, each 0.76 m in diameter. It was driven by a 5 hp dc motor with SCR controller. A dual belt and pulley drive system coupled the motor and the fan.

EXPERIMENTAL DESIGN

The phenomenon of heat transfer from a flat plate with a step change in surface temperature was selected for the study of turbulent temperature structure in the near-wall region of a turbulent boundary layer. This flow situation, with the velocity and temperature boundary layers, is illustrated in Fig. 1(b). The flat plate consisted of an unheated starting length and a heated portion, therefore, making the origins of momentum and thermal boundary layers different. The unheated starting length was 42.6 cm long with a leading edge sandpaper (60 GRIT, open coat, aluminum oxide) surface of 15.3 cm long for tripping the flow to ensure the presence of a two-dimensional boundary layer.

The heated portion of the flat plate consisted of 21 individually heated aluminum plates. The plates were 3.18 mm thick and came in two different sizes: 25.4 cm by 2.54 cm and 25.4 cm by 15.2 cm. They were separated from each other by 3.18 mm thick cork board to minimize axial heat conduction. The smaller sized plates were used to provide an accurate measurement of the surface heat transfer rate as a function of downstream position. They were distributed along the tunnel floor as shown in Fig. 2 of ref. [3]. Cork board and oak wood were used between the plates' ends and the side walls (Plexiglas).

The plates were heated by custom manufactured silicon rubber heating elements. The power input to each plate was controlled by commercially available rhotostat switches. The power input to the heating elements was calibrated against the root-mean-square (rms) voltage across the heating element. The current

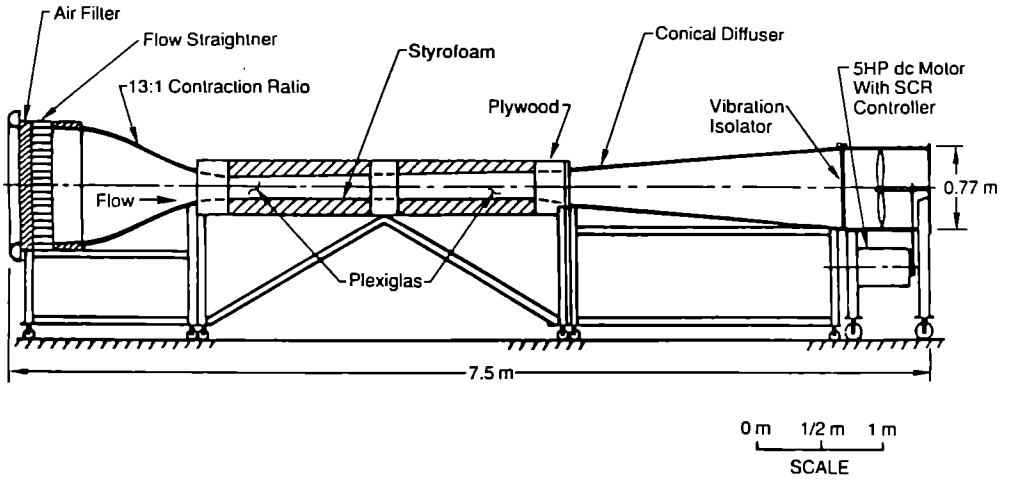

FIG. 1(a). Wind-tunnel facility

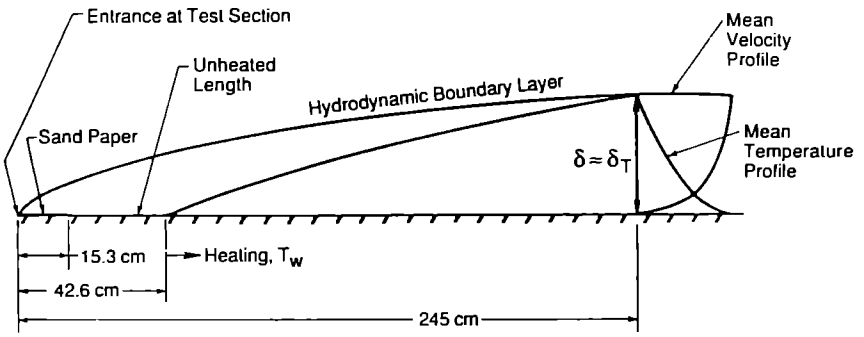

FIG. 1(b). Velocity and thermal boundary layers and their associated profiles.

input to the plates was drawn from a single voltage regulator to ensure uniform and constant power. The heating elements were placed adjacent and beneath the aluminum plates which were secured to wooden frames especially designed to minimize energy loss.

The heating elements were insulated from the bottom using various insulating materials. The insulating materials used were fiberglass ($k = 0.0484$ W m^{-1} K^{-1}), cork board ($k = 0.0433$ W m^{-1} K^{-1}), and styrofoam ($k = 0.0381$ W m^{-1} K^{-1}). The styrofoam, 5 cm thick, was used to insulate the bottom side of the test section. Seven pieces of fiberglass, each 0.361 cm thick, and four pieces of cork board, each 0.361 cm thick, were used to fill up the gap in each of the wooden frames so as to ensure insulation from the bottom. The composite insulation pieces were compressed from the top by securing the aluminum plates to the wooden frames to provide uniform contact between the aluminum plates and the heating elements.

The conduction heat losses from the bottom and the side walls and the radiation heat loss from the top surface of the plates for the three different temperature cases considered in this study were calculated and found to be a maximum of 3% of the heat input to the plates.

The wall or surface temperature of the aluminum plates was measured using type E miniature thermocouples having a diameter of 0.127 mm. This type of thermocouple consists of constantan–chromel wires. The wires were spotwelded at the junction.

The thermocouples were calibrated in a Rosemount Constant Temperature Bath against a Platinum Resistance Thermometer (PRT) for a range of 15–50°C temperatures. A Hewlett–Packard 3421A data-acquisition system with a HP 85 minicomputer were used to measure the voltage response of the thermocouples. This voltage was linearly correlated to the temperature of the thermocouples.

The measurement of the true surface temperature is an extremely difficult task. The difficulties arise from two different sources: heat loss from the thermocouple, i.e. natural convection and radiation; and, the way the thermocouple is attached to the surface [4]. Circular cavities (0.159 mm deep and 0.953 mm in diameter) were milled in the underneath side of the aluminum plates and the thermocouples were installed in the cavities. The thermocouples came to direct contact with the aluminum plates by sealing them with aluminum disks, made previously to fit the cavities. The advantages of this method are the elimination of natural convection and radiation losses and to mini-

mize the introduction of foreign materials between the thermocouples and the solid surface. With minor exceptions, the three thermocouples were embedded in each of the aluminum plates, one at the center and two at the opposite spanwise ends. The two lateral end points were positioned a distance of ± 8.25 cm from the center. Overall, 69 thermocouples were placed in the plates for surface temperature measurements. Two additional thermocouples were used to monitor the freestream and ambient temperatures. One was placed inside the test section for freestream temperature measurements and one was placed outside the test section for ambient temperature measurements.

Nine eight-channel-multiplexer-connector blocks were used to connect the thermocouples to the data-acquisition systems. Two model HP 3421A data-acquisition systems in conjunction with HP 85 and HP 86A minicomputers were used for surface temperature measurements. Three uniform wall-temperature differences of 10, 15 and 20 C were used for the experiments. A plot of the centerline wall-temperature distributions along the plate for the three temperature-difference cases is shown in Fig. 2. The wall temperatures were normalized with respect to the nominal temperature difference and show acceptable uniformity along the plate. For the 10, 15 and 20 C temperature difference cases, the wall temperatures were uniform within ± 0.2, ± 0.25, and ± 0.35 C, respectively. The temperature difference was the difference between the mean plate surface temperature and the freestream temperature. The freestream temperature was about 20 C and the wall temperatures were about 30, 35 and 40 C for the three temperature difference cases.

EXPERIMENTAL PROCEDURE AND MEASUREMENT TECHNIQUES

Velocity profiles

The measurements were made at a nominal freestream velocity of 17.5 m s^{-1} for the three different temperature cases. Table 1 lists some parameters of interest at the measurement station. Mean and fluctuating components of the streamwise velocity profiles were measured using hot-wire anemometry. A Thermo System Inc. (TSI) anemometer, model 1050, with a frequency response of 100 kHz was used. The anemometer was operated in the constant-temperature mode at an overheat ratio of 1.8. A TSI standard single-sensor boundary-layer probe, model 1218 T1.5, was used for both mean and fluctuating profile measurements. The sensor was a platinum-plated tungsten wire with a sensing diameter of 3.8 μm and a sensing length of 1.25 mm. The probe was connected to a DIGIMATIC, Mitutoyo Corporation, traversing mechanism having a spatial resolution of 10 μm, and traversed normal to the plate for the mean and fluctuating profiles.

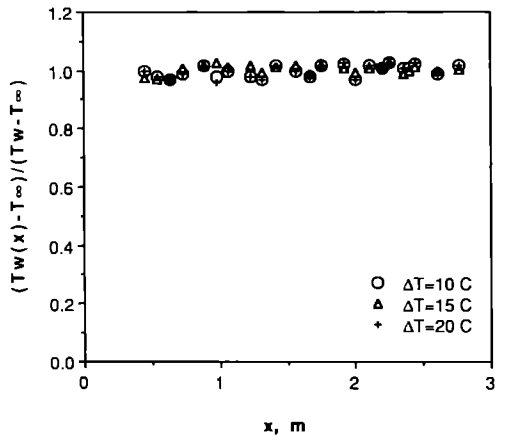

FIG. 2. Centerline wall temperature distribution.

Table 1. Experimental parameters at the measurement station

ΔT (C)	x (m)	$Re_x * 10^{-6}$	δ (mm)	θ (mm)	δ_T (mm)	$Re_{\Delta x}$	q_w (W)
10	2.45	2.84	45	4.7	38	3770	14.43
15	2.45	2.84	45	4.7	42	4540	21.50
20	2.45	2.84	45	4.7	45	4690	28.49

The anemometer signal was processed through a low-pass filter, Krohn-Hite model 3323, with a cutoff frequency of 2500 Hz and then measured with an IBM AT personal computer and IBM DACA board data-acquisition system. For each point of the velocity profiles, a total of 40 000 samples at a 10 000 Hz sampling rate were taken. This sampling frequency satisfies the Nyquist criteria for true rms measurements [5]. The cutoff frequency was determined after detailed analysis of the flow was made using a Nicolet-660A digital spectrum analyzer.

The hot-wire probe was calibrated in the wind tunnel in connection with a Pitot-static tube using a Meriam micromanometer. The variation in room temperature during the hot wire probe calibration was minimal, less than 0.5 C. The probe was calibrated in the range of 2.5–25 m s^{-1} freestream with the same cutoff frequency and overheat ratio values used for the velocity measurements. Approximately 20 data points were taken for each of the velocity calibration curves. A fourth-order polynomial then was fitted to each of the calibration profiles and their constant coefficients were determined using the least-square method.

Temperature measurements

Mean and fluctuating temperatures were measured using hot wire anemometer. A TSI model 1050 anemometer was used in constant current mode. The current was set at a value of 1.5 mA, recommended by TSI, which resulted in a very low overheat. A commercial TSI standard single sensor boundary layer probe, model 1218 T1.5, was used for mean tem-

perature profiles. This sensor is the same as that used for the velocity measurements.

A commercial TSI subminiature straight probe, model 1276 P.5, was used for fluctuating temperature profiles. The sensor is a platinum wire with a sensing diameter of 1 μm and a sensing length of 1 mm. This sensor provided extremely high sensitivity to temperature fluctuations because of its small thermal inertia. A special probe holder had to be designed for this subminiature probe for boundary layer temperature measurements. The cutoff frequency for temperature measurements was set at 2000 Hz. This cutoff frequency was determined after the flow was analyzed with the Nicolet power spectrum analyzer. Bagheri [6] reports on the results of the power spectrum curves as a function of temperature differences at different y^+ values. Each point of the temperature measurement was comprised of 40 000 samples sampled at 10 000 Hz.

The temperature probes were calibrated against a calibrated thermocouple in a heated stream provided by a modified commercial hair drier. The hair drier was modified such that its fan speed and its temperature could be controlled independently using a power supply and a variac, respectively. The detailed procedure for the cold wire probes' calibration for temperature measurements is given in Appendix V of Bagheri [6].

Two-point correlations

Two-point correlation measurements were made for the temperature fluctuations. Two temperature fluctuation probes, model 1276 P.5, were positioned at known longitudinal, normal, and lateral distances between the two probes. For the normal correlation one probe was held fixed at a y^+ value of 32 and the other probe was traversed to different y^+ positions. A total of 15 pair-correlation points were acquired for each temperature difference case. For the longitudinal and lateral correlations, a single probe was held fixed at a given y^+ value and the other probe was moved to different longitudinal, x^+, and/or lateral, z^+, positions for the same y^+ value. The reference heights for the streamwise correlation were set at y^+ values of 75, 175, and 425. For each height and each temperature difference case a total of five Δx^+ values ranging from 150 to 750 were measured. The reference height for the lateral correlation was set from y^+ values of 60 to the edge of the boundary layer where the y^+ value was about 1950. For each y^+ location, a total of nine different heights, and each temperature difference case an average of seven Δz^+ with values ranging from 75 to 1400 were taken. For each temperature probe and every measurement point a total of 60 000 samples at a sampling rate of 10 000 Hz were taken. The cutoff frequency for both probes was set at 2000 Hz.

For the lateral movements a special probe holder was designed and built to minimize flow disturbances. This probe holder had to have the capability of being moved laterally by sliding the holder in and out with respect to the test section, and at the same time registering the lateral movement with respect to a reference point. For this purpose a digital DIGIMATIC caliper, Model 500-351, was mounted on the holder so to register the lateral movement with an accuracy of 10 μm.

A Cyborg ISAAC-2000 data-acquisition system in conjunction with an IBM/AT personal computer was used for two-point correlation measurements. The ISAAC-2000 has a maximum frequency response of 200 kHz with eight channels with 312 K data-memory capabilities. The programming language 'C' was used for data-acquisition triggering. The data were written and stored on floppy disks, transferred to an IBM-9370 computer through the IBM emulation program, processed, and analyzed.

UNCERTAINTY ANALYSIS

The uncertainty caused by equipment accuracy and statistical calculations in this study was calculated. The standard approach presented by Kline and McClintock and described by Holman [7] was followed for uncertainty analysis of the mean quantities. The uncertainties were estimated with odds of 20:1. The statistical or random error uncertainties of the fluctuating quantities were estimated from the observed scatter in measurements as well as from the equations given by Bendat and Piersol [5]. The uncertainties associated with the skin-friction coefficient, C_f, and friction speed, u^*, were estimated from the range of reasonable straight line 'Clauser-type' fits to the mean velocity profile in the logarithmic core region. The results of the uncertainty estimates are listed in Table 2.

PRESENTATION OF RESULTS

The streamwise velocity profile measurements were used to check the maturity and growth of the hydrodynamic boundary layer, and to determine the local skin-friction coefficient distribution along the plate using the Clauser-chart method. Based on the velocity law-of-the-wall results the characteristics of the boundary layer were found to be two-dimensional and in equilibrium at the stations where measurements were taken. A typical universal mean velocity profile

Table 2. Typical uncertainty estimates

Variable	Uncertainty (%)
u	± 2.0
u^*	± 5.4
T	± 2.5
Re	± 2.5
C_f	± 3.4
St	± 5.0
u_{rms}	± 4.5
T_{rms}	± 5.0
$R_{T,T}$	± 1.3

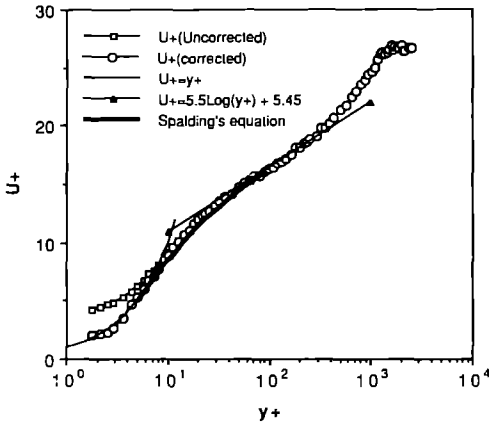

FIG. 3. Universal velocity-law-of-the-wall.

non-dimensionalized with respect to the friction velocity is shown in Fig. 3. The wall unit ν/u^* had a value of about 0.023 mm. The near-wall region velocity data were corrected to account for the wall effects. Wills' [8] correction method was used for the hot-wire data in the near-wall region. Corrections were applied to a y^+ value of about 14. Wills' corrected and uncorrected data along with Spalding's law-of-the-wall equation may be observed in Fig. 3. The heat-conducting wall caused higher voltage drop across the hot-wire sensor which resulted in higher velocities. The error in the hot-wire signal diminished as the distance away from the wall was increased. At a y^+ value of 14 no effect of the heat-conducting wall was observed. The velocity data in the logarithmic core region fit very closely the law-of-the-wall equation given by Patel [9], which is

$$u^+ = 5.5 \log y^+ + 5.45. \quad (1)$$

Additionally, the spanwise velocity profile measurements were used to check the two-dimensionality of the flow. At the measurement station, 2.45 m from the leading edge, the maximum spanwise variation of velocity was less than $\pm 1.5\%$ and occurred within the boundary layer where the local turbulence level was greater than 8% [6]. Spanwise variation in the momentum-deficit Reynolds number was less than $\pm 1\%$.

Correlation measurements

In this study, for the space–time correlation measurements, two temperature fluctuation probes were used to measure the temperature fluctuations simultaneously at two points in the spatial–temporal space. The two probes were positioned at known longitudinal, normal, and spanwise spatial distances between the two probes. The turbulent signals from the two probes were then obtained and correlated for the three temperature difference cases.

The temperature cross-correlation coefficient is defined as

$$R_{T,T} = T(x, y, z, t)T(x+\Delta x, y+\Delta y, z+\Delta z, t+\Delta t)/ [T_{\rm rms}(x, y, z)T_{\rm rms}(x+\Delta x, y+\Delta y, z+\Delta z)] \quad (2)$$

where T is the temperature fluctuations; $T_{\rm rms}$ the root mean square value of T; (x, y, z) the location of one probe in space; $(\Delta x, \Delta y, \Delta z)$ the separation of the second probe from the first probe; t the time coordinate and Δt the variable time shift. This cross-correlation coefficient is a measure of the similarity between the two temperature fluctuation signals. This means that at a given spatial distance between the two probes, the two probes observed the same or two similar structures; however, the observed features have been altered due to the flow field dynamics when they reach the second probe. The extent of similarity between the two signals depends on the absolute value of the cross-correlation coefficient. A high absolute value means that the two signals are highly correlated and are thought to be similar. The maximum absolute value of a correlation coefficient is equal to unity which is the correlation value of a signal being correlated with itself; called an auto-correlation value. The auto-correlation coefficient can be calculated from the cross-correlation coefficient when $\Delta x = \Delta y = \Delta z = 0$.

Turbulent momentum and heat transport across a turbulent boundary layer are thought to be similar; however, the degree of similarity is not known. Since this transport of momentum and heat is associated with the turbulence structure near the wall, knowledge of the flow structure in that region of the flow is required. As mentioned before, this has been done in detail for isothermal flows. The same isothermal flow analysis for determining large-scale structure characteristics is now applied to a non-isothermal turbulent boundary layer flow.

Convection velocity

The mean convection velocity of the temperature fluctuations was obtained from the correlation measurements in the streamwise direction ($\Delta y = \Delta z = 0$). Two temperature probes were positioned at different streamwise spacings and the same heights. The reference heights were set at y^+ values of 75, 175, and 425 to get a distribution of the mean convection velocity of the T' structure. For each height and each temperature difference case a total of five Δx^+ values were taken. The space–time correlations of temperature fluctuations for the 10, 15, and 20°C temperature difference values and the three reference heights are shown in Figs. 4(a)–(i). Each figure contains the space–time correlations at the same height and different streamwise spacings between the probes.

From the space–time correlation measurements, the time shifts of the peak $R_{T,T}(\Delta x^+)$ correlation values from the zero time axis were measured for the three temperature difference cases. These time shifts, temporal displacements, are created by the passage of turbulent temperature fluctuation eddies which move

with a convection velocity which is some fraction of the freestream velocity. The results of the spatial displacement vs the temporal displacement are shown in Figs. 5(a)–(c) for the three heights and three temperature difference cases. The temporal displacements vary linearly with the streamwise separation and appear to be independent of the temperature difference. The slope of each line, $\mathrm{d}x/\mathrm{d}t = U_c$, gives an estimate of the convection velocity of the temperature fluctuations at the given height.

Figure 6 shows the variation of the mean convection velocity with height. On the same figure the local mean

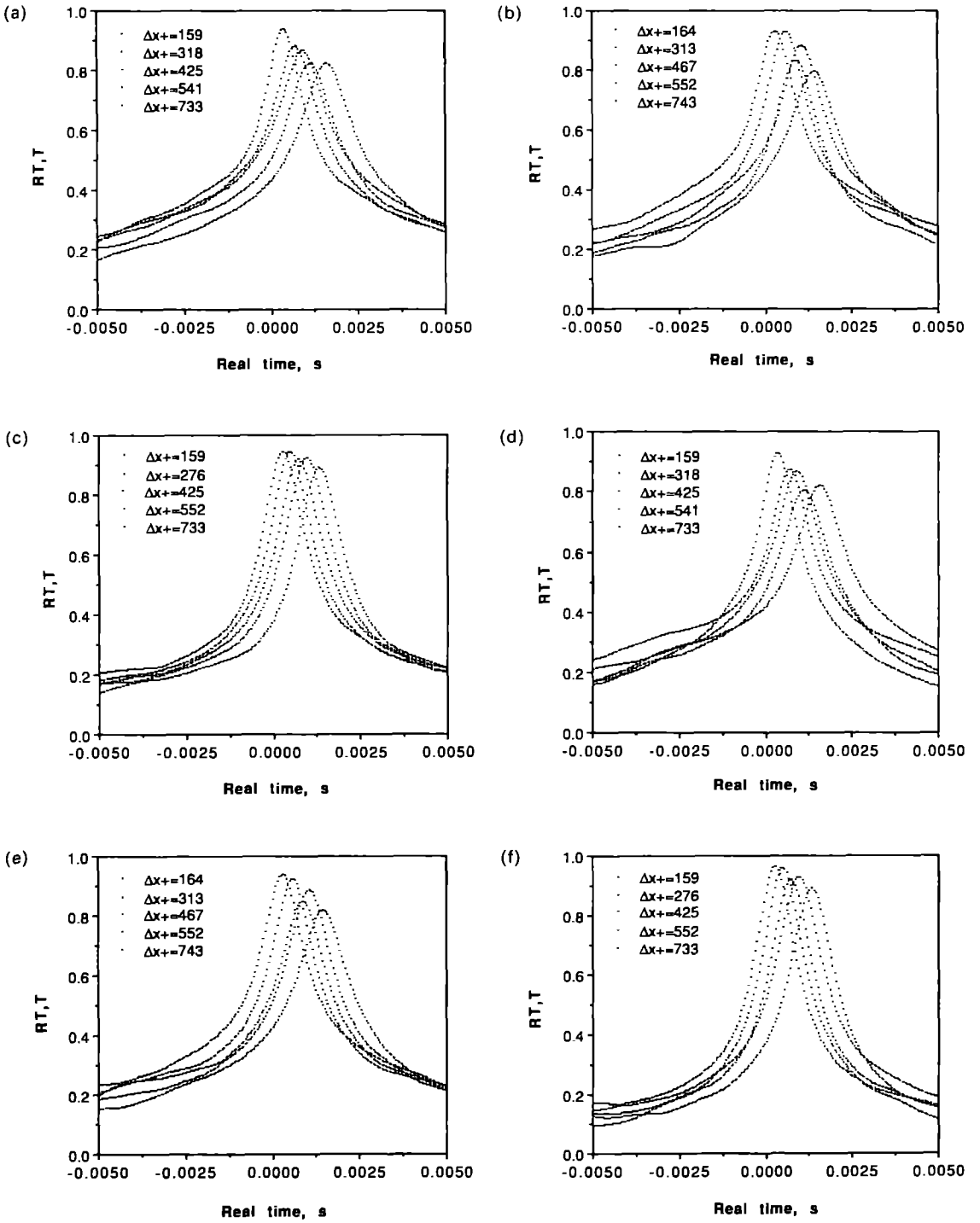

FIG. 4. Streamwise correlations: (a) $\Delta T = 10°C$, $y^+ = 75$; (b) $\Delta T = 10°C$, $y^+ = 175$; (c) $\Delta T = 10°C$, $y^+ = 425$; (d) $\Delta T = 15°C$, $y^+ = 75$; (e) $\Delta T = 15°C$, $y^+ = 175$; (f) $\Delta T = 15°C$, $y^+ = 425$; (g) $\Delta T = 20°C$, $y^+ = 75$; (h) $\Delta T = 20°C$, $y^+ = 175$; (i) $\Delta T = 20°C$, $y^+ = 425$.

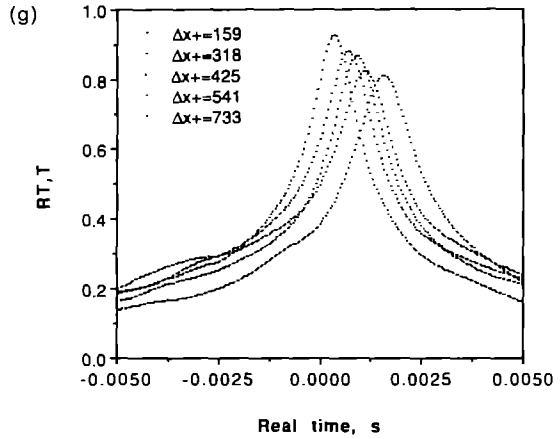

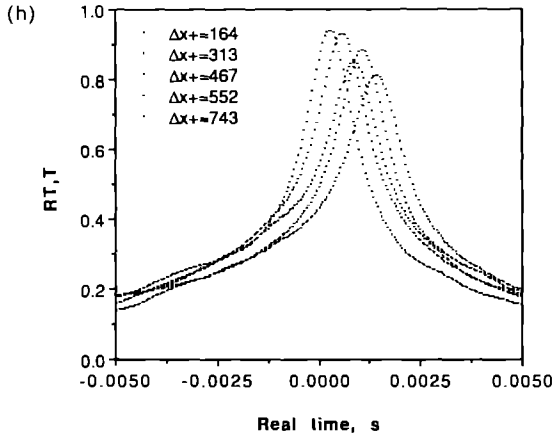

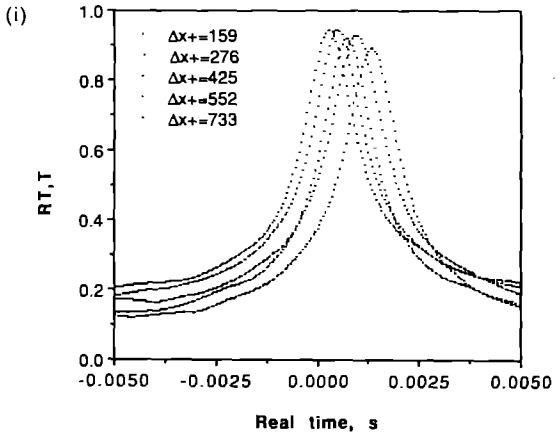

FIG. 4.—*Continued.*

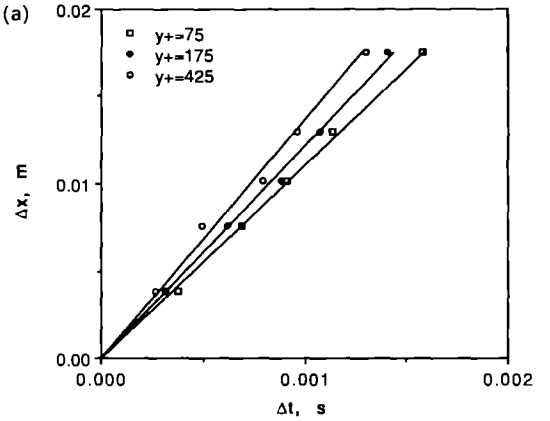

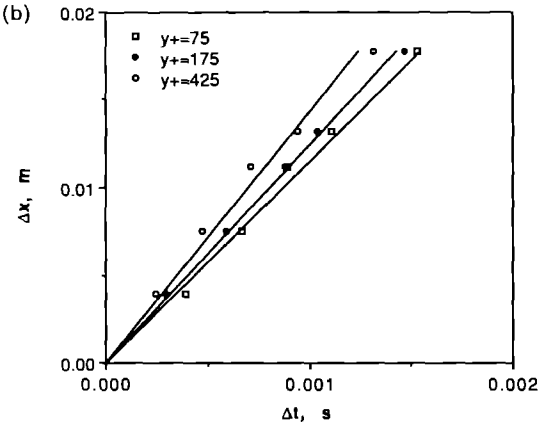

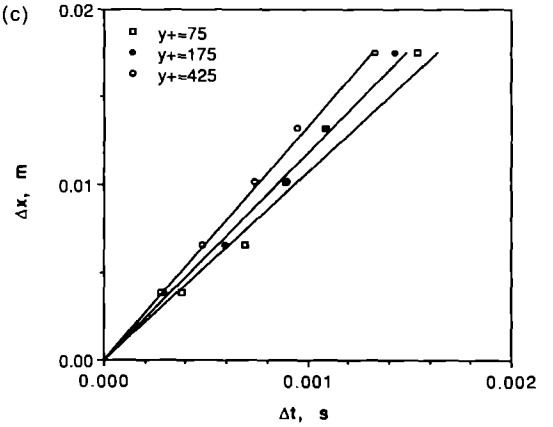

FIG. 5. Convection velocity determination: (a) $\Delta T = 10°C$; (b) $\Delta T = 15°C$; (c) $\Delta T = 20°C$.

velocity is also shown. The convection velocity of the T' structure varies approximately from $0.65u_\infty$ at $y^+ = 75$ to $0.77u_\infty$ at $y^+ = 425$. For the isothermal turbulent boundary layer flow Strataridakis *et al.* [2] measured the convection velocities of the u', v', and $u'v'$ structures. For the convection velocity of the u' structure Strataridakis *et al.* reported variations approximately from $0.25u_\infty$ at $y^+ \approx 12$ to $0.8u_\infty$ at $y^+ \approx 150$. For the convection velocity of the v' and $u'v'$ structures they found that the convection velocity of both structures remained invariant with height and were equal to about $0.8u_\infty$. A comparison of the convection velocity of the present data with the Strataridakis *et al.* data suggests that the convection velocity of the T' structure is more closely related to the convection velocity of the u' structure, although

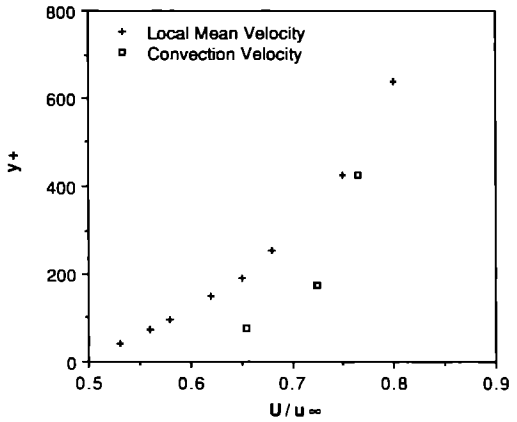

FIG. 6. Mean convection velocity variation.

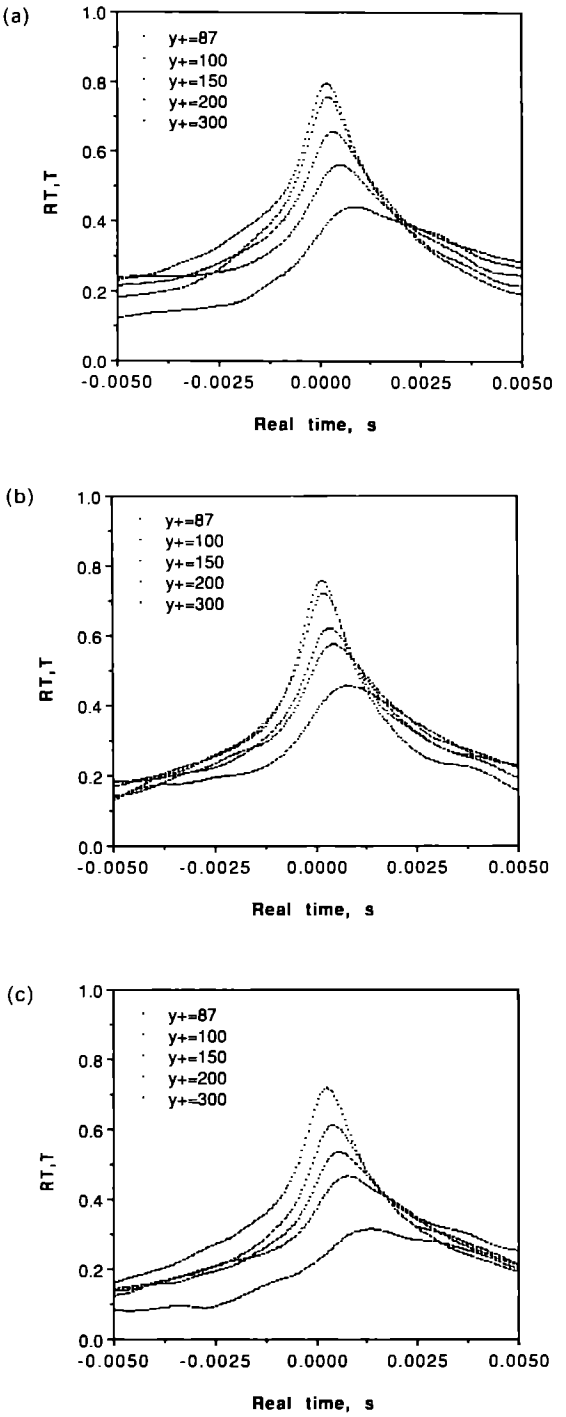

FIG. 7. Normal correlations at different heights of the traversed probe: (a) $\Delta T = 10^{\circ}$C; (b) $\Delta T = 15^{\circ}$C; (c) $\Delta T = 20^{\circ}$C.

not identical to it, than the v' structure. The convection velocity of the u' structure of the Strataridakis *et al.* data was equal to 25% of the freestream at $y^+ \approx 12$. The lowest height considered in the present study for the evaluation of the convection velocity was at a $y^+ = 75$ which resulted in a T' structure convection velocity of 65% of the freestream. The Strataridakis *et al.* data for the u' structure convection velocity reached 80% of the freestream at $y^+ \approx 150$. This 80% value is believed to be the maximum percentage of the freestream velocity reported in studies made on isothermal turbulent boundary layer flows. The convection velocity of the T' structure of the present study reached 77% of the freestream velocity at $y^+ = 425$. This y^+ value is higher than the corresponding level of the u' structure.

Inclination angle

The mean inclination angle of the temperature fluctuations was obtained from the correlation measurements in the normal direction ($\Delta x = \Delta z = 0$). Two temperature probes were positioned at different normal spatial distances. One probe was held fixed at a reference height of $y^+ = 32$, and the other probe was traversed to different y^+ positions. The traversing probe was positioned at several points within the turbulent boundary layer. The normal correlation measurements were made for all the three temperature difference cases.

From the space–time correlation measurements the time shifts, temporal displacements, of the peak $R_{T,T}(\Delta y^+)$ correlation values from the zero time axis were measured. Figures 7(a)–(c) show some typical space–time correlations at different traversed probe heights for the three temperature difference cases. The figures show relatively high correlation values of 0.72–0.75 at the peaks for a y^+ value of 100. The values of the time shifts, along with the convection velocity $U_c(y^+)$, were used to estimate the streamwise extent of the structure Δx^+ using Taylor's hypothesis, i.e.

$$\Delta x^+ = U_c \Delta t u^*/v. \quad (3)$$

The ensembled results of the three temperature difference cases are shown in Fig. 8. It is observed that the average inclination angle of the temperature fluctuation structure is inclined to the wall at about 30° and appears to be relatively independent of the limited temperature difference cases. This inclination angle is within the range of inclination angles of

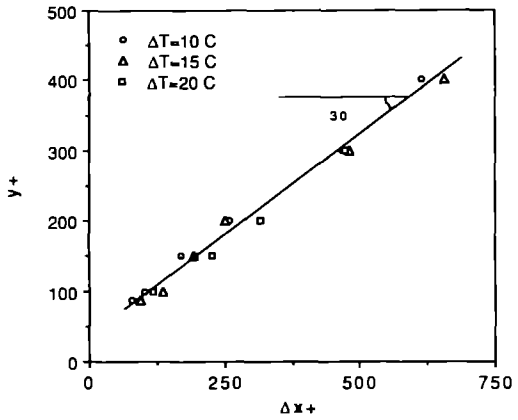

FIG. 8. Mean inclination angle of the T' structure.

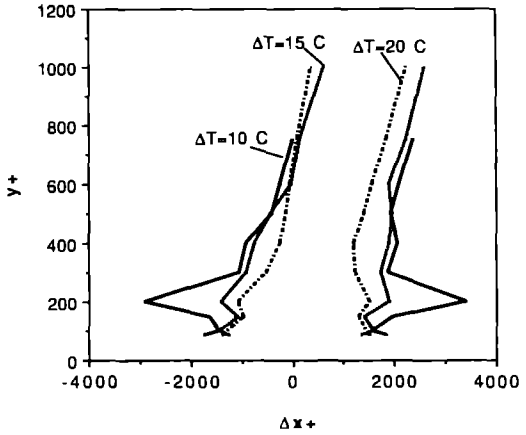

FIG. 9. Isocorrelation contour, streamwise view.

streamwise velocity fluctuations for isothermal flows observed by many other investigators, i.e. Brown and Thomas [10], Strataridakis *et al.* [2], and others. For the isothermal turbulent boundary layer flow Strataridakis *et al.* reported an average inclination angle of 17° for the u' structure, when the fixed probe was held at a reference height of $y^+ = 12$. For the same structure, when the reference height was set at $y^+ = 40$, they observed an average inclination angle of 19°. The small decrease in inclination angle when the reference height decreases might indicate that the 'back' of the structure is evolving as it travels downstream due to variation of the convection velocity of the structure with height. Strataridakis *et al.*, therefore, concluded that the structure-back profile depended slightly on the reference height, y^+. The dependency of the structure-back profile on reference height could not be addressed in the present study since only one reference height was considered for the mean inclination angle of the T' structure. Comparison of the inclination angle of the present data with the data of Strataridakis *et al.* suggests that the inclination angle of the T' structure is more closely related to the inclination angle of the u' structure than the v' structure.

Space–time correlation contours

The extent of the $R_{T,T}$ isocorrelation contours with a constant value of 0.3 is shown in Fig. 9. The figure shows the streamwise view of the structure at $\Delta z^+ = 0$ for the three temperature difference cases. The $R_{T,T} = 0.3$ value is felt to be the lower limit at which coherence is present between the measurements of the probes for the present experimental set-up.

The streamwise extent of the T' structure is slightly dependent (for $y^+ < 400$) on the temperature difference value and decreases as temperature difference is increased. The T' structures for the three temperature difference cases appear to be widest at a y^+ value of about 200. For the temperature difference case of 10°C the structure extends up to $\Delta x^+ \approx 3\delta^+$ at the value of $y^+ \approx 200$ whereas the 15 and 20°C temperature difference cases extend up to, at the same y^+ value, $\Delta x^+ \approx 2\delta^+$ and $1.5\delta^+$, respectively. Normal to the wall, the extent of the T' structures is of the order of δ^+. The smaller size of the T' structure for higher temperature difference values suggests that the temperature fluctuations of those structures are less coherent than the temperature fluctuations of the structures of a lower temperature difference value.

For the isothermal turbulent boundary layer flow, Strataridakis *et al.* reported a streamwise extension of $\Delta x^+ \approx 3\delta^+$ for the u' structure. For the v' structure they reported a much narrower structure in the same direction. In the normal direction they reported that the normal extent of the u' and v' structures are of the order of δ^+ and $2\delta^+$, respectively. Comparison of the streamwise view of the spatial extent of the T' structure of the present data with the data of Strataridakis *et al.* suggests that the spatial extent of the T' structure is more closely related to the u' structure than the v' structure, in both the streamwise and normal spatial extents.

From the correlation measurements in the spanwise direction, the spanwise view of the T' structure was obtained. Figures 10(a)–(c) show these structures for the three temperature difference cases. The spanwise extent of the structure is of the order of δ^+ and slightly decreases as the temperature difference increases when the isocontour level of 0.1 is considered in all the figures. The isocorrelation contours of the 20°C temperature difference case in the near-wall region have smaller extent than the isocorrelation contours of the 10 and 15°C temperature difference cases. In other words, the isocorrelation contours of the 20°C temperature difference are more closely spaced than the other two temperature difference cases. This suggests that the T' large-scale structure of the 20°C temperature difference case may be associated with smaller size eddies than the 10 and 15°C temperature difference cases in the near-wall region. The same conclusion may also be made from consideration of Fig. 9 in which the extent of the T' structure is smaller

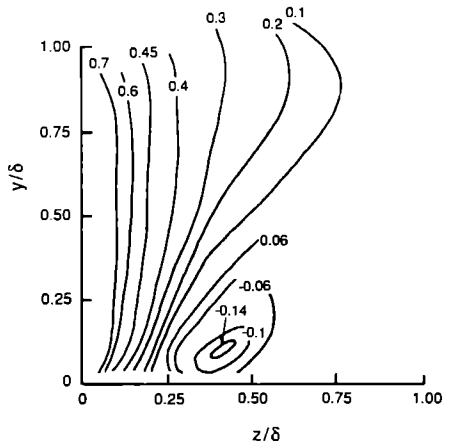

FIG. 10(a). Spanwise view of the isocorrelation contours; $\Delta T = 10$ C.

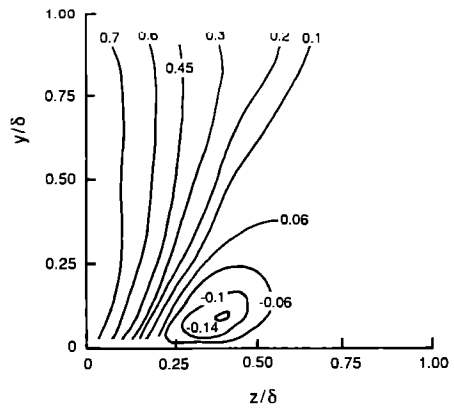

FIG. 10(b). Spanwise view of the isocorrelation contours; $\Delta T = 15$ C.

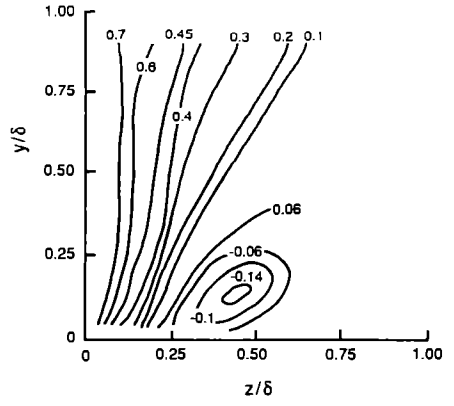

FIG. 10(c). Spanwise view of the isocorrelation contours; $\Delta T = 20$ C.

for higher values of the temperature difference. For the isothermal turbulent boundary layer flow, Strataridakis *et al.* reported a spanwise extension of $\Delta z^+ \approx \delta^+$ for both u' and v' structures. This result is consistent with the present data that the spanwise extent of the T' structure is of the order of δ^+.

Negative isocorrelation contours were observed in all the spanwise isocorrelation contours for the three temperature difference cases. These negative regions were centered at $y^+ \approx 200$ and $\Delta z^+ \approx 0.4\delta^+$ for all the temperature difference cases. Strataridakis *et al.* also observed weakly negative correlation regions for both u' and v' structures. They found that these regions are centered at $y^+ \approx \delta^+/2$ and $\Delta z^+ \approx \delta^+/2$. These centers of negative isocorrelation contours occurred at a greater value of y^+ than the center of the negative isocorrelation contours of the present work. This lower center of negative correlation region suggests that the near-wall T' structure of the non-isothermal turbulent boundary layer flows have smaller extent, smaller eddy sizes, than the near-wall u' structure of the isothermal flows.

CONCLUSIONS

Space–time correlations of the temperature fluctuations, mean convection velocity of the large-scale structures, and isocorrelation contours were measured for a turbulent incompressible zero-pressure-gradient boundary-layer flow with a heated uniform wall temperature for three temperature-difference cases between the wall and the freestream.

The mean convection velocity of the temperature fluctuation structures was determined to vary from $0.65u_\infty$ at $y^+ = 75$ to $0.77u_\infty$ at $y^+ = 425$ and appeared to be independent of the limited temperature difference cases considered. The convection velocities were determined from the correlation measurements in the streamwise direction. The convection velocity of the T' structure was found to be closely related to the convection velocity of the u' structure. The convection velocity of the u' structure of isothermal flows considered in other investigations, i.e. Strataridakis *et al.*, reached 80% of the freestream velocity at a y^+ value much smaller than the corresponding 80% level of the convection velocity of the T' structure.

The mean inclination angle of the temperature fluctuation structure was determined to be 30 to the wall and independent of the limited temperature difference cases considered in this study. The mean inclination angle was obtained from the correlation measurements in the normal direction. The value of the inclination angle was found to be within the range of inclination angles of streamwise velocity fluctuations for isothermal flows observed by other investigators [2, 10]. From comparisons made with the isothermal flow inclination angle, it was determined that the inclination angle of the T' structure was more closely related to the inclination angle of the u' structure than the v' structure.

The streamwise extent of the T' structure was determined to be slightly dependent on the temperature difference value. The spatial extent of the T' structure decreased as the temperature difference value was increased. For the temperature difference cases of 10, 15, and 20°C the maximum streamwise spatial extent,

Δx^+, of the T' structure was found to be of the order of $3\delta^+$, $2\delta^+$, and $1.5\delta^+$, respectively. The normal and spanwise spatial extent of the T' structure of the three temperature difference cases were found to be of the order of δ^+. From the isocorrelation contours of the T' structure it was determined that the T' large-scale structure of the 20 C temperature difference case was associated with smaller size eddies than the 10 and 15 C temperature difference cases. The maximum extent of the T' structure-coherence was observed to occur at $y^+ \approx 200$ compared to a value of $y^+ \approx \delta^+/2$ for the u' structure of isothermal flows.

Negative isocorrelation contours were observed in all the spanwise isocorrelation contours. The center of these regions was determined to be at a lower height y^+ than the center of negative isocorrelation contours of the u' structure of the isothermal flows. The negative regions were centered at $y^+ \approx 200$ and $\Delta z^+ \approx 0.4\delta^+$ compared to $y^+ \approx \delta^+/2$ and $\Delta z^+ \approx \delta^+/2$ for the u' structure of isothermal flows. The lower y^+ height of the center of negative correlation region suggests that the T' structures have smaller spatial extent than the u' structure in the near-wall region of the boundary layer.

In summary, from the correlation results, mean convection velocity, mean inclination angle, and spatial extent of the T' structure, it is suggested that the temperature fluctuation structures of the present non-isothermal flow are more similar to the u' structure than the v' structure of the flows.

Acknowledgements—This work would not have been possible without the assistance and workmanship of the personnel of the Electrical General Services, Mr Bill Weigt and Mr Larry Gage, and the Mechanical General Services, Mr Don Barnum, Mr Bill Zeller, Mr Leo Palaima, and Mr Jerry Dill.

REFERENCES

1. S. J. Kline and S. K. Robinson, Quasi-coherent structures in the turbulent boundary layer: part I. Status report on a community-wide summary of the data, *Zoran P. Zarić Memorial International Seminar on Near-wall Turbulence*, Dubrovnik, Yugoslavia, 16–20 May (1988).
2. C. J. Strataridakis, B. R. White and S. K. Robinson, Experimental measurements of large scale structures in an incompressible turbulent boundary layer using correlated X-probes, AIAA-89-0133 (1989).
3. N. Bagheri, C. J. Strataridakis and B. R. White, Turbulent Prandtl number and space–time temperature correlation measurements in an incompressible turbulent boundary layer, *AIAA J.* **30,** 35–42 (1992).
4. A. Berukhim, Heat transfer measurements in turbulent boundary layer, MS Thesis, University of California, Davis, California (1986).
5. J. S. Bendat and A. G. Piersol, *Random Data* (2nd Edn). Wiley Interscience, New York (1986).
6. N. Bagheri, Turbulent Prandtl number and space–time temperature correlation measurements in an incompressible turbulent boundary layer, Ph.D. Thesis, University of California, Davis, California (1989).
7. J. P. Holman, *Experimental Methods for Engineers* (3rd Edn). McGraw-Hill, New York (1978).
8. J. A. B. Wills, The correction of hot-wire readings for proximity to a solid boundary, *J. Fluid Mech.* **12,** 388–396 (1962).
9. V. C. Patel, Calibration of the Preston tube and limitations on its use in pressure gradients, *J. Fluid Mech.* **23,** 185–208 (1965).
10. G. L. Brown and A. S. W. Thomas, Large structures in a turbulent boundary layer, *Physics Fluids Suppl.* **20,** Part II, 243–252 (1977).